Clin. Lab. 2026;72:XXX-XXX

ORIGINAL ARTICLE

In Vitro and In Silico Evidence for Arak Extract as a Potent Inhibitor of NO/iNOS in Activated Macrophages

Marwa M. Ellithy [1], Abdulrahman M. Saleh [2], Mohamed N. Ibrahim [3], Saleha Y. M. Alakilli [4], Eman Fawzy El-Azab [3]

[1] *Basic Dental Science Department, National Research Center, Giza, Egypt*
[2] *Pharmaceutical Medicinal Chemistry and Drug Design Department, Faculty of Pharmacy (Boys), Al-Azhar University, Cairo, Egypt*
[3] *Clinical Laboratories Department, College of Applied Medical Sciences, Jouf University, Qurrayat, Kingdom of Saudi Arabia*
[4] *Department of Biological Sciences, Faculty of Sciences, King Abdulaziz University, Jeddah, Kingdom of Saudi Arabia*

SUMMARY

Background: **The anti-inflammatory properties of Arak (Miswak, Salvadora persica) and its extracts have been firmly established through both *in vitro* and in silico studies. Nitric oxide (NO) plays a critical role as a signaling molecule in the pathogenesis of inflammation, which is a fundamental process in the development of various diseases, particularly carcinogenesis and the malignant transformation of cells. Herbal-derived compounds have demonstrated promising potential in inhibiting inflammatory diseases. This study aimed to investigate the inhibitory effects of Arak extract and its bioactive compounds on inducible nitric oxide synthase (iNOS) and NO production using vitro and computational methods and to identify potential phytocompounds with high binding affinity to iNOS.**

Methods: **An *in vitro* evaluation was performed using LPS-stimulated RAW macrophage cell lines to assess the inhibitory effect of Arak extract on NO production. Additionally, advanced in silico techniques, including all-atom molecular dynamic (MD) simulations, were used to model the interaction between six phytocompounds and iNOS, identify binding sites, and assess the stability and conformational shifts of the ligand-protein complexes.**

Results: **The *in vitro* analysis revealed strong inhibition of NO production by Arak extract. Computational studies confirmed that six bioactive compounds from the extract exhibited high binding affinity to iNOS, inducing conformational changes that enhanced ligand positioning within the active site. Among these, the compound 1/iNOS complex showed stable ligand interactions over the simulation period, suggesting a robust inhibitory effect.**

Conclusions: **This study highlights six promising phytocompounds from Arak extract as potent iNOS inhibitors. The results demonstrate the therapeutic potential of Arak in treating inflammation-related diseases. Further *in vivo* validation is warranted to confirm the clinical efficacy of these findings.**

(Clin. Lab. 2026;72:xx-xx. DOI: 10.7754/Clin.Lab.2025.250505)

Correspondence:
Mohamed Nabil Ibrahim, PhD
Clinical Laboratory Science Department
College of Applied Medical Sciences
Qurrayat, Jouf University
Kingdom of Saudi Arabia
Phone: + 966 562698734
Email: mnabil@ju.edu.sa

Manuscript accepted June 17, 2025

KEYWORDS

arak, inflammation, iNos, MD simulation, molecular docking, NO

INTRODUCTION

Inflammation is a critical response that occurs when agents capable of inducing infection, including bacteria, viruses, or fungi, invade the human body and enter the bloodstream. Furthermore, inflammation can be triggered by tissue injury, cell death, cancer, ischemia, and

degeneration. It serves as a vital protective mechanism, effectively restoring cell function and facilitating tissue repair [1]. However, it is important to recognize that the inflammatory mediators released can also result in significant tissue damage and necrosis, particularly in cases of chronic, long-standing inflammation. Immune cells - specifically neutrophils, monocytes, and macrophages - are the primary producers of these inflammatory mediators, with nitric oxide (NO) being one of the key players in the inflammatory process [2].

Bacterial infections and immunological stimuli, such as lipopolysaccharide (LPS), interferon-γ (IFN-γ), or interleukin-1, trigger the expression of inducible nitric oxide synthase (iNOS), leading to the production of large amounts of nitric oxide (NO) [1]. In pathological conditions, immune cells, especially macrophages, increase their production of NO and superoxide anions. This leads to the formation of peroxynitrite (ONOO-), which enhances oxidative damage of cells with irreparable DNA damage [2]. Excess levels of NO can be cytotoxic, harming surrounding cells and contributing to severe conditions such as septic shock, cerebral injury, myocardial ischemia, and various inflammatory disorders and diseases [3]. Therefore, inhibiting iNOS expression and activity is a crucial therapeutic goal for treating allergic and immunological pathologies, as well as persistent inflammatory conditions.

Nitric oxide (NO), produced by inducible nitric oxide synthase (iNOS), plays a significant role in causing DNA damage and disrupting normal cell signaling in various tissues. [4]. iNOS synthesizes NO from L-arginine and plays a role in several biological processes. In the context of infectious diseases, human macrophages express iNOS, which enables them to eliminate various microbes [5]. In chronic inflammatory and autoimmune diseases, elevated levels of iNOS and NO are present in conditions such as rheumatoid arthritis, multiple sclerosis, asthma, and type 1 diabetes. These elevated levels are also found in cancers of the breast, lung, prostate, and colon. In the oral cavity, increased iNOS mRNA levels are observed early in neoplastic development [6]. Research in rats has shown that the selective iNOS inhibitor S, S-1,4-phenylene-bis(1,2-ethanediyl) bis-isothiourea can stop neoplastic progression in the esophagus, indicating that iNOS could be a potential therapeutic target. NO and related nitrogen species promote carcinogenesis by inducing DNA damage and impairing DNA repair enzymes through a process called nitrosation [7].

NF-κB serves as a key regulator of iNOS, as multiple κB-binding sites are present in its promoter, while AP-1 is also involved in its regulation. Additionally, NO acts as a powerful cell signaling molecule, activating NF-κB through tyrosine modification and stimulating AP-1 via ERK activation [8].

While modern medicine boasts significant advancements, around 80% of the global population relies on traditional remedies from nature, mainly due to financial barriers that limit access to expensive pharmaceuticals. [9]. For centuries, the healing properties of plant oils and extracts have been undeniably recognized, especially in their ability to combat inflammation. There is a growing body of scientific evidence that shows the potent anti-inflammatory effects of various plants [10].

Arak chewing sticks are not just a trend; they are a vital part of Arab culture. Sourced from the *Arak tree (Salvadora persica),* predominantly found in Saudi Arabia and the Middle East, these sticks are integrated into many dental products due to their powerful antiplaque and antimicrobial properties [11]. *Arak* is essential for oral health, leveraging its mechanical action and rich chemical composition. Key compounds, such as tannins, effectively reduce plaque, while resins offer robust protection against cavities. Furthermore, its array of detectable substances contributes to its notable antimicrobial, anti-inflammatory, and antioxidant properties.

The World Health Organization (WHO) endorses its use for promoting oral health, cementing its value in dental care [11].

In the field of molecular modeling, docking is a technique that predicts how a ligand interacts with a target molecule to form a stable complex [12].

Molecular dynamics (MD) is a computer simulation method used to analyze the physical movements of atoms and molecules. In this approach, atoms and molecules interact over a fixed period, allowing us to observe the dynamic "evolution" of the system [12].

This paper decisively evaluates the anti-inflammatory properties of ethanolic arak extract, establishing it as a promising source for medicinal products. This study intended to evaluate the potential of *arak* ethanolic extract on NO inhibition in LPs stimulated RAW macrophages *in vitro*. In addition, molecular docking and MD simulation for iNOS binding site were performed for the major compounds found in *Arak* extract.

Our findings will serve as crucial benchmark for arak compounds in relation to iNOS, paving the way for the development of innovative and highly effective anti-inflammatory drugs.

MATERIALS AND METHODS

Chemicals and reagents

Arak extract was purchased from Nawah Research Laboratories, Mokattam, Egypt.

LPS from Escherichia coli, SRB, dimethyl sulfoxide (DMSO), Griess reagent, sodium nitrite, protease inhibitor cocktail, and phosphate-buffered saline (PBS) were obtained from Sigma-Aldrich (St. Louis, MO, USA). Dulbecco's modified Eagle's medium (DMEM), antibiotics (penicillin/streptomycin solution), and fetal bovine serum (FBS) were obtained from Thermo Fisher Scientific (Waltham, MA, USA).

Cell culture and maintenance

The RAW 264.7 cells, mouse macrophage cell line, were obtained from Nawah Scientific Inc. (Mokatam,

Cairo, Egypt). Cells were maintained in DMEM media supplemented with 100 mg/mL of streptomycin, 100 units/mL of penicillin, and 10% of heat-inactivated fetal bovine serum in humidified, 5% (v/v) CO2 atmosphere at 37°C.

Cell cytotoxicity and IC 50 calculation

Cell viability was assessed by SRB assay. Aliquots of 100 µL cell suspension (5 x 10^3 cells) were spread in 6-well plates and incubated in complete media for 24 hours (Figure 1a). Cells were treated with another aliquot of 100 µL media containing drugs at various concentrations. After 72 hours of drug exposure, cells were fixed by replacing media with 150 µL of 10% TCA and were incubated at 4°C for 1 hour. The TCA solution was removed, and the cells were washed 5 times with distilled water. Aliquots of 70 µL SRB solution (0.4% w/v) were added and incubated in a dark place at room temperature for 10 minutes. Plates were washed 3 times with 1% acetic acid and were allowed to air-dry overnight. Then, 150 µL of TRIS (10 mM) were added to dissolve protein-bound SRB stain; the absorbance was measured at 540 nm using a BMG LABTECH®-FLUOstar Omega microplate reader (Ortenberg, Germany).

Anti-inflammatory assay (NO production)

RAW 264.7 cells were seeded into a 96-well plate and incubated for twenty-four hours. The next day, inflammation was induced with 1 µg/mL of LPS (LPS-group), and untreated cells were replenished with fresh media (Control group). Compounds were treated with LPS in five concentrations (LPS + 50, 100, 200, and 300 µg/mL). Quercetin (30 uM) was used as an anti-inflammatory positive control (Figure 1b).

To measure nitric oxide (NO) secretion, equal volumes of the cell supernatant and Griess reagent were mixed for 10 minutes in the dark at room temperature. Thereafter, the cell supernatant and Griess reagent (1% sulfanilamide, 0.1% N-1-(naphthyl) ethylenediamine dihydrochloride, 2.5% phosphoric acid) were mixed in a 1:1 ratio and incubated for 20 minutes. Absorbance was measured at 540 nm using a microplate reader (Tecan, Mannedorf, Switzerland). The amount of NO produced was quantitatively calculated using the standard curve of sodium nitrite ($NaNO_2$). Concentrations were calculated by comparison with OD550 of standard solutions of sodium nitrite prepared in culture medium.

Statistical analysis

Cytotoxicity results and NO were expressed as mean ± SD from three independent experiments in Microsoft Office Excel.

Molecular docking

To study the molecular binding of Arak extract with iNOS protein, MOE2014 software was used to evaluate the possible affinity of the tested compounds against inducible nitric oxide synthase (iNOS). The target proteins (code: 4ux6) were obtained from the protein data bank [1] (Table 1). At first, water molecules were removed from the complexes. Next, preparation options were used to prepare and correct crystallographic disorders and unfilled valence atoms. Protein structure energy was minimized by applying CHARMM force fields; hence, defining and preparing the pockets for the docking process. By using Chem-Bio Draw Ultra17.0, 2D structures of tested compounds were drawn and saved as SDF files. The saved files were opened, 3D structures were protonated, and 0.1 RMSD kcal/mole energy was minimized by the MMFF94 force field. Then, the minimized structures were prepared for docking via the ligand preparation tools. The docking process was carried out through the docking option using MOE2014 [2]. The receptor was held rigid while the ligands were allowed to be flexible. During the refinement, each molecule was allowed to produce twenty different poses with the proteins. Then, docking scores (affinity energy) of the best-fitted poses with the active sites were recorded, and the Discovery Studio 2016 visualizer generated 3D figures [3].

Method of MD simulation

The Desmond simulation package from Schrödinger LLC was utilized for conducting molecular dynamic (MD) simulations [1]. The NPT ensemble, with a temperature set at 300 K and a pressure of 1 bar, was consistently employed across all runs. The simulations ran for 100 ns, with a relaxation time of 1 ps for the tested ligands. OPLS_2005 force field parameters were employed for all simulations. Long-range electrostatic interactions were computed using the particle mesh Ewald method, with a cutoff radius of 9.0 Å for Coulomb interactions [2].

Water molecules were explicitly represented using the simple point charge model. Pressure control utilized the Martyna-Tuckerman-Klein chain coupling scheme with a coupling constant of 2.0 ps, while temperature control employed the Nosé-Hoover chain coupling scheme. Non-bonded forces were calculated using an r-RESPA integrator, with short-range forces updated every step and long-range forces updated every three steps. Trajectories were saved at 4.8 ps intervals for subsequent analysis.

The behavior and interactions between ligands and proteins were examined using the Simulation Interaction Diagram tool within the Desmond MD package. The stability of MD simulations was assessed by monitoring the root mean square deviation (RMSD) of ligand and protein atom positions over time.

Additionally, the AMBER 14 package [3], with the AMBER force field ff99, was employed for various tasks, including minimization, addition of counterions, solvation, equilibration, and running periodic box, explicit water (TIP4P) MD simulations for the tested ligands. The structures of the tested ligands were optimized using the density functional theory B3LYP method with a 6-31G basic set, and parameters were set to

Table 1. Chemical structure of compounds contained in *arak* extract.

Array	Structure	Common name
Flavonoids		
Compound 1	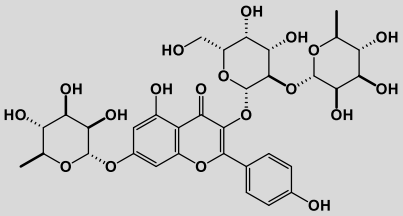	**3-(((2S,3R,4S,5R,6R)-4,5-dihydroxy-6-(hydroxymethyl)-3-(((2S,3R,4R,5R,6S)-3,4,5-trihydroxy-6-methyltetrahydro-2H-pyran-2-yl)oxy)tetrahydro-2H-pyran-2-yl)oxy)-5-hydroxy-2-(4-hydroxyphenyl)-7-(((2S,3R,4R,5R,6S)-3,4,5-trihydroxy-6-methyltetrahydro-2H-pyran-2-yl)oxy)-4H-chromen-4-one**
2	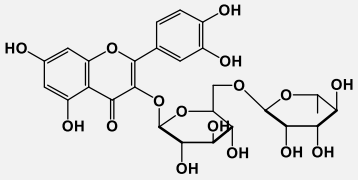	**Rutin**
3	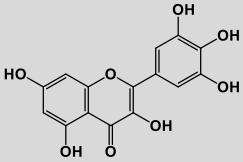	**Myricetin**
4	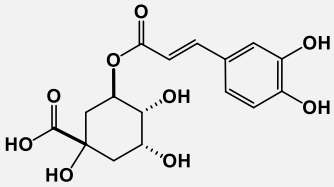	**Chlorogenic acid**
Alkaloids		
5	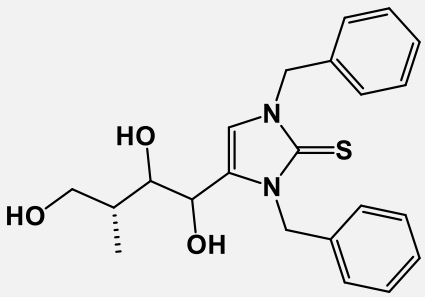	**Persicaline**

the GAFF force field. The protein-ligand-water system was allowed to move freely during simulations, which comprised 10 independent runs with different random initial velocities. Each run spanned 10 ns, utilizing a timestep of 0.001 ps (1 fs). Multiple MD simulations, widely recognized for their robustness, can provide more adequate sampling of conformational space than longer single-trajectory simulations.

Data analysis was conducted using the cpptraj program from the AMBER Tools distribution.

RESULTS

Cytotoxicity results

In this study, it was found that ethanolic *arak extract* has moderate cytotoxic potential, with an IC50 concentration of 260 µg/mL in cell cytotoxicity statistical data. Notably, *arak extract* exhibited non-toxicity on RAW 264.7 cells up to a concentration of 200 µg/mL, where cell viability exceeded 70% (mean cell viability = 84.77). Increasing miswak extract concentration leads to a directly proportional cytotoxic effect. At 300 µg/mL, miswak extract is remarkably cytotoxic to RAW cells

Table 2. Results of molecular docking of natural candidates extracted from *Arak* against inducible nitric oxide synthase (iNOS).

Target	Tested compound	RMSD value (Å)	Docking (affinity) score (kcal/mol)	Interaction	
				H.B	π -interaction
Inducible nitric oxide synthase (iNOS)	chlorogenic acid	1.08	-8.01	4	2
	persicaline	1.76	-8.10	3	5
	compound 1	1.47	-9.27	7	6
	myricetin	0.75	-8.08	5	2
	rutin	1.50	-8.14	6	4
	co-crystalized ligand	1.07	-8.12	3	5

Table 3. MM-GBSA energy for compound 1/iNOS complex (kcal/mol).

Compound 1	ΔG_Bind	Coulomb	Covalent	H-bond	Lipo	vdW
At 100ns	-90.91	-30.08	28.5	-2.85	-52.26	-34.22

Coulomb Coulomb energy, Lipo lipophilic energy, H-bond hydrogen bonding energy, VdW Van der Waals energy.

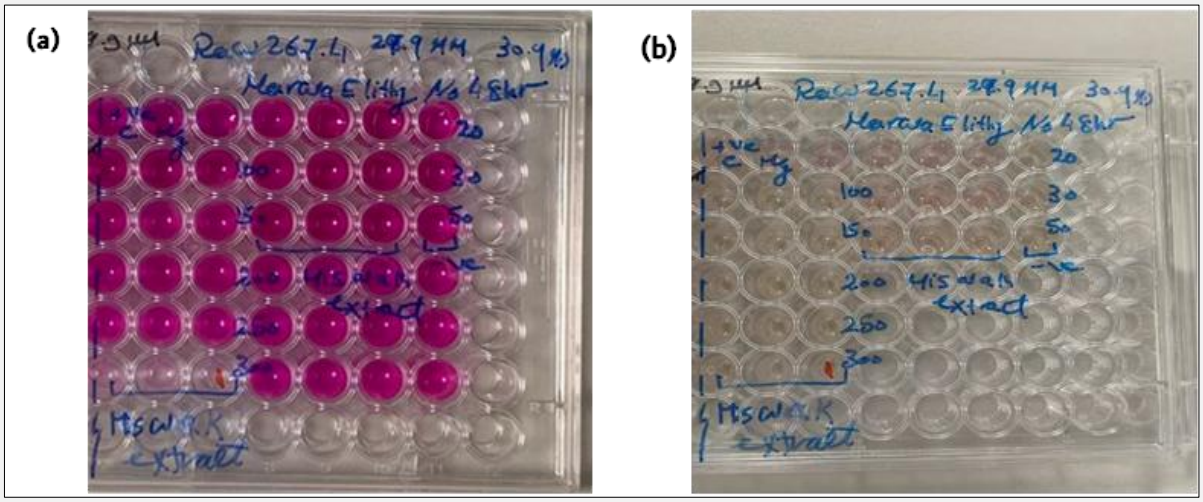

Figure 1. 96 well plate a) showing SRB cytotoxicity assay and b) showing nitric oxide assay.

(mean cell viability = 1.063). So, in subsequent experiments, the maximum concentration of arak extract used was 100 µg/mL. As a result, concentrations less than or equal to 100 µg/mL were used for the anti-inflammatory assay.

Arak extract inhibits NO production

The investigation assessed the concentration of nitric oxide (NO) in RAW 264.7 cells after stimulation with lipopolysaccharide (LPS) at 1 µg/mL both on its own and in combination with various concentrations of arak (ranging from 0 to 100 µg/mL). Quercetin was included

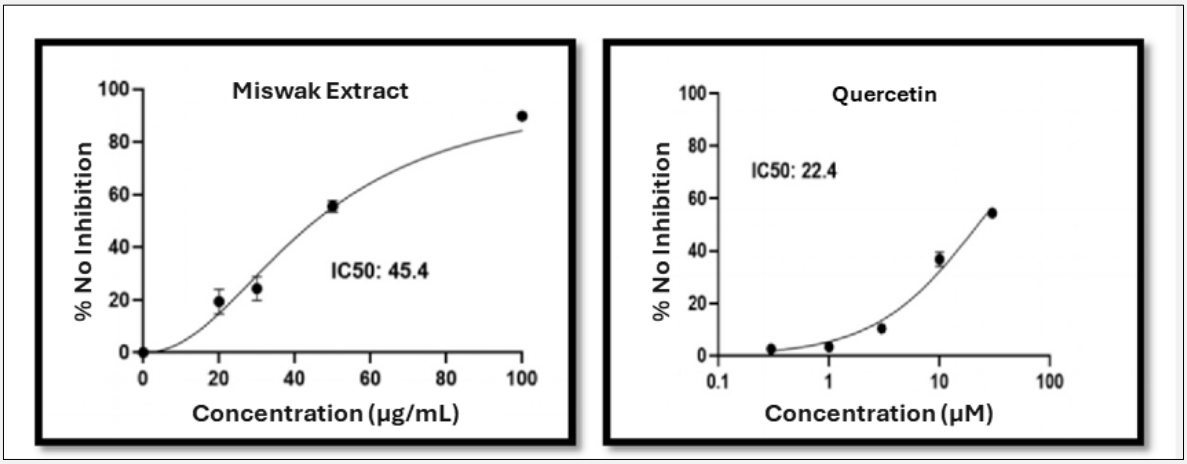

Figure 2. NO inhibition in RAW cells using Arak extract.

as positive control due to its known ability to inhibit NO production. Nitric oxide (NO) production was influenced by the activation state of the cells. Unstimulated macrophages, after 48 hours of culture, produced the lowest levels of NO. The addition of Arak extract did not significantly alter the baseline NO production. Even at a concentration of 100 µg/mL, the NO levels in the medium remained comparable to those of the unstimulated samples. Stimulating the cells with LPS (1 µg/mL) for 24 hours significantly increased nitric oxide (NO) production from the basal level of 0% NO inhibition. In these experiments, arak extract (0 - 100 µg/mL) consistently demonstrated a concentration-dependent inhibition of NO production (Figure 2). The half-maximal inhibitory concentration (IC50) of miswak for inhibiting nitrite production was precisely 45.5 µg/mL. Notably, significant inhibition by arak was achieved at a concentration of 75 µg/mL, and an impressive inhibition of over 80% was observed at 100 µg/mL.

NO production was inhibited, and this was proved by the decrease in total % from 100% in LPS alone-induced cells to 50% at the concentration of 45.5 µg/mL. At 150 µg/mL, miswak extract inhibited NO significantly with a mean of 89% inhibition. This shows the potential of arak extract in inhibiting inflammatory responses.

Molecular docking results

As shown in Table 2, the binding mode of chlorogenic acid and persicaline against inducible nitric oxide synthase (iNOS) exhibited binding energy equal to -8.01, and -8.10 kcal/mol, respectively. Chlorogenic acid formed two hydrophobic π-Alkyl interactions with Val 346, and Cys194, additionally interacted with Ser256, Ile195, and Met368 by four hydrogen bonds with distances of 2.91, 2.33, 2.60, and 2.52 Å (Figure 3a), while persicaline interacted with Cys194, Val346, Met349, and Glu371 by five hydrophobic π-Alkyl, π-sulfur, and π-anion interactions. On the other hand, three hydrogen bonds were observed with Gln257, Glu371, and Ile195, with distances of 2.12, 1.89, and 2.85 Å, respectively (Figure 3b).

The binding mode of Compound 1 against inducible nitric oxide synthase (iNOS) exhibited a binding score equal to -9.27 kcal/mol, respectively. Compound 1 interacted with Met114, Trp457, Trp188, Pro344, and Val346 by six hydrophobic π-alkyl interactions and was supported by seven hydrogen bonds with Arg375, Gln257, Thr367, Cys194, and Gly196, with distances of 2.88, 1.74, 2.91, 2.14, 1.75, and 2.49 Å (Figure 3c).

The binding mode of myricetin and rutin against inducible nitric oxide synthase (iNOS) exhibited binding energy equal to -8.08, and -8.14 kcal/mol, respectively. Myricetin formed two hydrophobic π-alkyl and π-anion interactions with Pro344 and Glu371, and additionally interacted with Arg382, Asp376, Tyr341, Trp366, and Met368 by five hydrogen bonds, with distances of 2.70, 2.56, 2.81, 2.66, and 2.23 Å (Figure 3d). While Rutin showed strong interaction with Gln381, Glu371, Gln257, Trp366, and Gly365 by six hydrogen bonds, with distances of 2.78, 1.79, 2.10, 1.97, 2.72, and 2.56 Å, respectively, four hydrophobic π-π and π-alkyl interactions were additionally noted with Arg193, Trp457, Val346, and Pro344 (Figure 3e).

The co-crystallized ligand of inducible nitric oxide synthase (iNOS) was redocked at the same pocket to validate the docking process; it exhibited an affinity score of -8.21 kcal/mol. The co-crystallized ligand formed

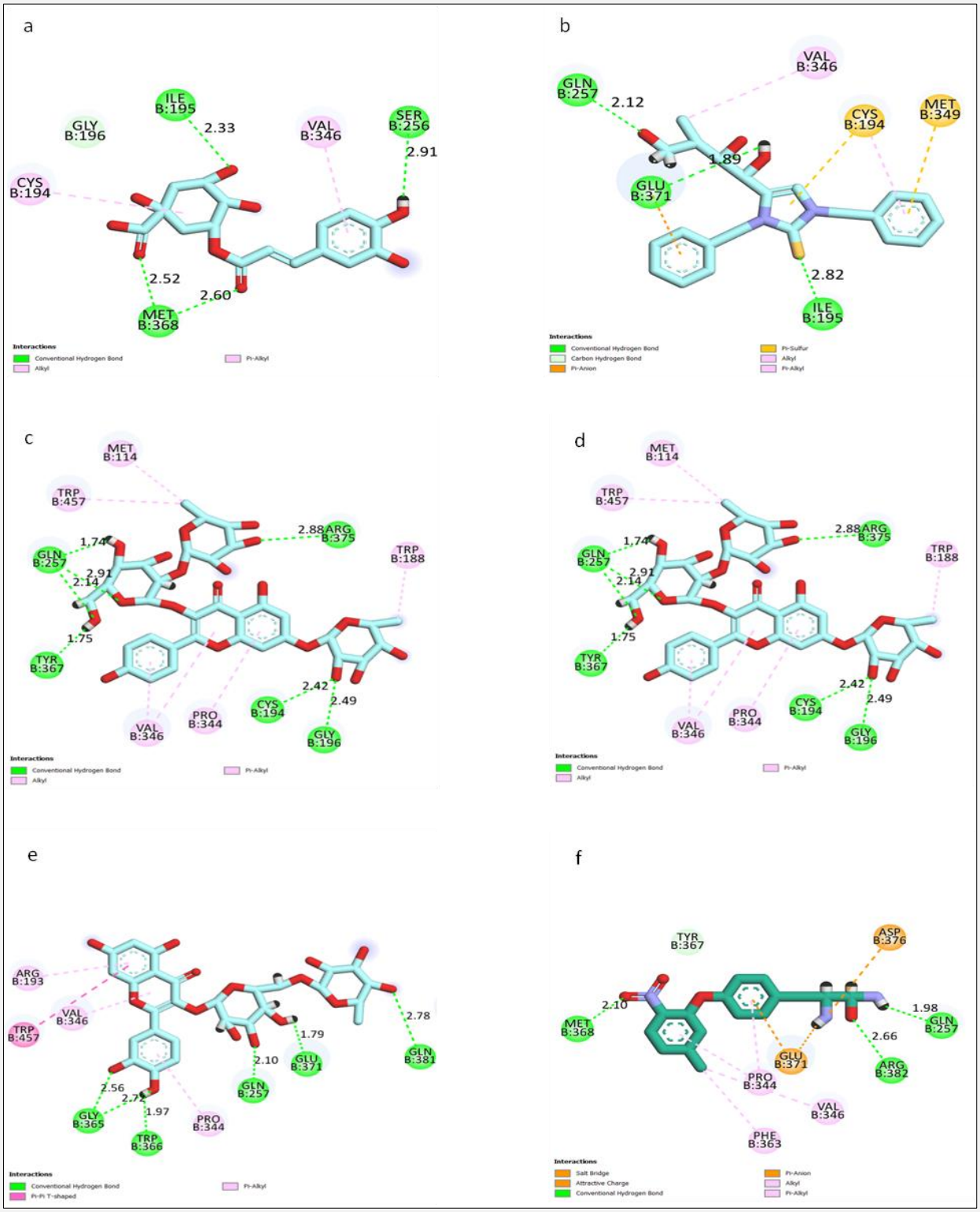

Figure 3. a) Chlorogenic acid/ligand. b) Persicaline/ligand. c) Compound 1/ligand. d) Myrecetin/ligand. e) Rutin/ligand. f) Co-crystallized/ligand.

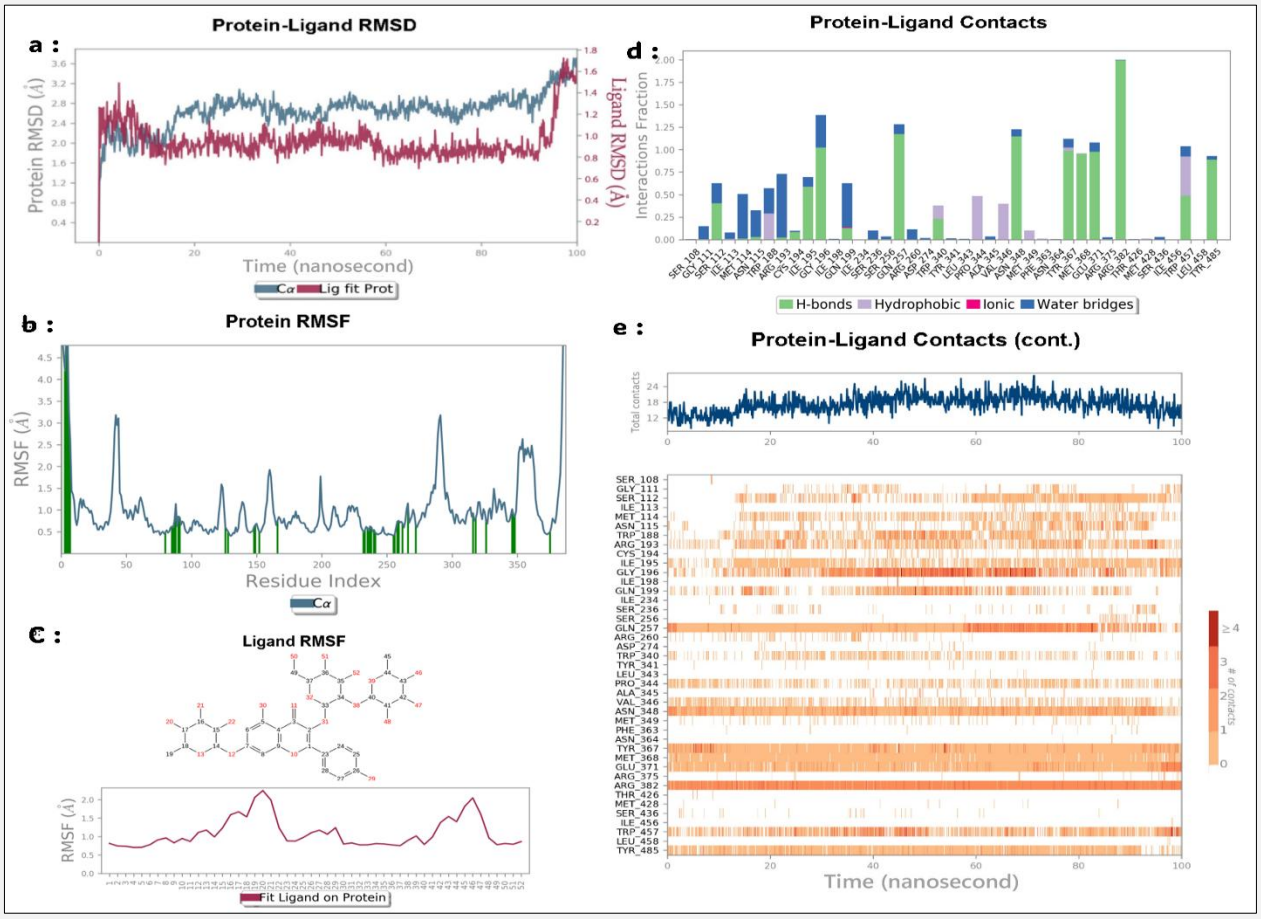

Figure 4. a) The RMSD of compound1/INOS complex for 100 ns. b) The RMSF of protein structure of INOS during simulation period. c) The RMSF of compound 1 during simulation period. d) Histogram describing the binding interactions of compound 1/INOS complex during the simulation time (100 ns). e) Heat map describing the total number of interactions within Compound 1/INOS complex during the 100 ns.

five hydrophobic π-interactions and two attractive ionic interactions with Phe363, Pro344, Val346, Glu371, and Asp376, and additionally interacted with Met368, Arg382, and Gln257 by three hydrogen bonds, with distances of 2.10, 2.66, and 1.98 Å (Figure 3f).

Based on previous results, *Arak* extract exhibited a promising affinity for the iNOS target site. Around twenty-seven candidates were evaluated to identify the best-fitting compounds for the target pocket. The flavonoid component of *Arak* extract showed the highest affinity among the compounds, fitting well within the target pocket and forming numerous hydrogen bonds and hydrophobic interactions. Compound 1, myricetin, and rutin demonstrated the highest affinity among the flavonoids. Additionally, phenolic acids, such as chlorogenic acid, also interacted with the target pocket similarly to flavonoids.

Molecular dynamic (MD) simulation

The root-mean-square deviation (RMSD) is essential for quantitatively analyzing how much each complex deviates from its initial position, which helps assess the overall stability of the system over the simulation period. The RMSD value of the comp1/(iNOS) complex is shown in Figure 4a. As illustrated in Figure 4b, the target protein (Cα) exhibited a stable RMSD of approximately 2.8 Å, indicating that the protein structure is stable and experiences low levels of conformational change. According to the root-mean-square fluctuation (RMSF) data for the protein structure (Figure 4c), some minor fluctuations were noted around the 50 and 300 amino acid regions, but no major fluctuations were observed throughout the entire simulation period. By examining the initial position of the ligand within the binding pocket of (iNOS), the ligand's RMSD was analyzed as a function of the 100 ns simulation time.

Histogram and heatmap of binding analysis

Compound 1 showed many interactions with INOS active pocket; about fourteen H-bonds were observed with the following residues: Ser112 (~ 40%), Asn115 (~ 5%), Arg193 (~ 5%), Cys194 (~ 10%), Ile195 (~ 60%), Gly196 (~ 110%), Gln199 (~ 15%), Gln257 (~ 130%), Trp340 (~ 25%), Asn348 (~ 120%), Tyr367 (~ 115%), Met368 (~ 115%), Glu371 (~ 115%), Arg382 (~ 200%), Trp457 (~ 45%), and Tyr485(~ 80%), as presented in Figure 4d.

Another type of H-bond interaction is the water-bridged H-bond, where crystal water molecules form a link between the protein residues and ligands. Compound 1 formed water-bridged H-bonds with residues Gly111 (~ 20%), Ser112 (~ 20%), Met114 (~ 75%), Asn115 (~ 25%), Arg193 (~ 70%), Gly196 (~ 20%), Gln199 (~ 50%), and Arg260 (~ 15) (Figure 4b). Additionally, compound 1 was able to form hydrophobic π-interactions with residues Trp188 (~ 20%), Trp340 (~ 15%), Pro344 (~ 45%), Val346 (~ 40%), Met349 (~ 65%), and Trp457 (~ 50%). Another method used to monitor these interactions involves plotting the number of interactions with respect to time; a heatmap (Figure 4e) indicates the number of interactions at each frame of compound 1/ iNOS complex, whereas the dark color indicates more interactions. From the heatmap, it was observed that the highest number of conformations of the protein formed up to twenty-four interactions between compound 1 and iNOS target site.

MM-GBSA calculations

We employed molecular mechanics, alongside generalized Born and surface area solvation (MM-GBSA), to effectively calculate the binding strain and free energy of docked ligands over a 100 ns period. The analysis yielded critical data, including ΔG binding energy, Coulomb energy, covalent energy, hydrogen bond energy, lipophilic energy, and van der Waals energy. The results obtained are described in Table 3.

As demonstrated in Table 3, the compound 1/iNOS complex exhibits a robust MM-GBSA binding energy of approximately -90.01 kcal/mol, which confirms an excellent fit for compound 1 within the iNOS target pocket. This finding unequivocally validates the strong inhibitory potential of the extracted compounds from Arak against the iNOS receptor, underscoring their effectiveness as powerful anti-inflammatory agents.

DISCUSSION

People are decisively turning to nature for effective solutions to various ailments. Therefore, herbal products have emerged as a powerful alternative to chemical remedies. Herbal medicines and preparations, which consist of plant components known for their therapeutic benefits, are superior to conventional drugs in many aspects. They offer proven natural efficacy, a higher safety margin, and lower costs. In the oral cavity, as an example, this shift is essential to sidestep the adverse effects linked to modern chemical therapeutics, such as the side effects of antibiotics, which include tooth and tongue discoloration and taste alterations. Also, this reduces the financial strain caused by expensive medications [11].

The World Health Organization (WHO) emphatically urges developing nations to utilize therapeutic herbs as essential components of their healthcare systems [12]. Natural tooth cleaning methods, such as chewing sticks from various plant parts, are not only effective but also widely practiced due to their accessibility and affordability. Salvadora persica, known as miswak, stands out as the "miracle twig," powerfully demonstrating the significant health benefits that nature provides [13,14].

Nitric oxide (NO) is an important regulator of inflammation, especially during acute responses. It is produced by inducible nitric oxide synthase (iNOS), which plays a crucial role in inflammation and sepsis [15]. Elevated levels of NO are associated with serious health conditions, including atherosclerosis, circulatory shock, diabetes, chronic inflammation, and cancer [16]. The three types of nitric oxide synthase - neuronal (nNOS), inducible (iNOS), and endothelial (eNOS) - highlight the importance of iNOS in effectively regulating NO levels during inflammatory processes. Molecular docking analysis has shown that key components of arak – myricetin, rutin, and chlorogenic acid - interact with iNOS, suggesting that arak extract has anti-inflammatory effects that target NF-κB pathways.

The compound 1/iNOS complex demonstrated a high binding energy of approximately -90.01 kcal/mol, indicating strong potential as an anti-inflammatory agent. In contrast to molecular docking, which provides a static representation of binding, molecular dynamic (MD) simulations offer insights into the dynamic behavior of protein-ligand interactions and assess their stability over time [17].

In accordance with the presented work, Gadnayak et al. (2024) conducted a computational study to identify four potential bioactive compounds with higher binding affinity to iNOS within the essential oils of C. angustifolia [12].

Molecular docking is a powerful tool for pinpointing ligand binding sites within a protein's active site; however, it neglects the crucial conformational changes that occur in the protein due to these interactions [18-20]. In our study, we conducted an in-depth analysis of molecular dynamic (MD) trajectories to precisely evaluate both the stability of these interactions and the resultant conformational adjustments of the protein. We confidently determined the protein's stability by calculating the backbone root mean square deviation (RMSD) from its initial conformation. Our results clearly indicate that the binding of phytocompounds to inducible nitric oxide synthase (iNOS) receptors does not result in any significant local conformational changes, as evidenced by the root mean square fluctuation (RMSF) patterns. Notably, four specific compounds consistently interacted with the

protein, underscoring their strong potential as effective therapeutic candidates for inflammatory disorders.
By employing bioinformation techniques akin to molecular docking and molecular dynamic (MD) simulation, Cheng et al. established that Genistein effectively regulates HDL cholesterol (HDL-C) and possesses anti-atherosclerotic properties. This action is clearly associated with the regulation of LIPC, CETP, and APOA1, leading to significant improvements in lipid metabolism [21].

CONCLUSION

The anti-inflammatory properties of arak/miswak extracts have been conclusively demonstrated through *in vitro* and in silico studies. Nitric oxide (NO) is established as a critical signaling molecule in the inflammatory response. Compounds derived from arak extract exhibit significant potential for inhibiting various inflammatory diseases. Our research confirms that bioactive elements in miswak extract effectively inhibit iNOS using advanced computational methods. Molecular dynamic simulations have clearly identified a crucial binding site on iNOS, allowing ligands to reposition within the binding interface. This study underscores promising bioactive compounds from arak extract that exhibit high binding affinity to iNOS. Further *in vivo* validation will firmly establish these novel compounds as effective anti-inflammatory agents for human diseases.

Acknowledgment:
The authors gratefully acknowledge the National Research Center and Cairo University, Egypt.

Source of Funds:
The authors received no financial support for the research, authorship, and/or publication of this article.

Declaration of Interest:
The authors have no competing interests to declare that are relevant to the content of this article.

References:

1. Kilbourn R, Griffith O. Overproduction of nitric oxide in cytokine-mediated and septic shock. J Natl Cancer Inst 1992 Jun 3; 84(11):827-31. (PMID: 1375655)

2. Ischiropoulos H, Zhu L, Chen J, et al. Peroxynitrite-mediated tyrosine nitration catalyzed by superoxide dismutase. Arch Biochem Biophys 1992 Nov 1;298(2):431-7. (PMID: 1416974)

3. Wu C, Thiemermann C. Biological control and inhibition of induction of nitric oxide synthase. Methods Enzymol 1996;268: 408-20. (PMID: 8782607)

4. Vakkala M, Kahlos K, Lakari E, Pääkkö P, Kinnula V, Soini Y. Inducible nitric oxide synthase expression, apoptosis, and angiogenesis in in situ and invasive breast carcinomas. Clin Cancer Res 2000 Jun;6(6):2408-16. (PMID: 10873093)

5. Marrogi AJ, Travis WD, Welsh JA, et al. Nitric oxide synthase, cyclooxygenase 2, and vascular endothelial growth factor in the angiogenesis of non-small cell lung carcinoma. Clin Cancer Res 2000 Dec;6(12):4739-44. (PMID: 11156228)

6. Aaltoma SH, Lipponen PK, Kosma VM. Inducible nitric oxide synthase (iNOS) expression and its prognostic value in prostate cancer. Anticancer Res 2001 Jul-Aug;21(4B):3101-6. (PMID: 11712818)

7. Chen T, Nines RG, Peschke SM, Kresty LA, Stoner GD. Chemopreventive effects of a selective nitric oxide synthase inhibitor on carcinogen-induced rat esophageal tumorigenesis. Cancer Res 2004 May 15;64(10):3714-7. (PMID: 15150132)

8. Jones LE Jr, Ying L, Hofseth AB, et al. Differential effects of reactive nitrogen species on DNA base excision repair initiated by the alkyladenine DNA glycosylase. Carcinogenesis 2009;30: 2123-9. (PMID: 19864471)

9. Azab A, Nassar A, Azab AN. Anti-inflammatory activity of natural products. Molecules 2016;21:1321. (PMID: 27706084)

10. Saleem TM, Azeem AK, Dilip C, Sankar C, Prasanth NV, Duraisami R. Anti-inflammatory activity of the leaf extracts of Gendarussa vulgaris Nees. Asian Pac J Trop Biomed 2011;1(2):147-9. (PMID: 23569746)

11. Abdelmagyd HAE, Shetty SR, Al-Ahmari MMM. Herbal medicine as adjunct in periodontal therapies: A review of clinical trials in past decade. J Oral Biol Craniofac Res 2019;9(3):212-7. (PMID: 31193290)

12. Gadnayak A, Nayak A, Jena S, et al. Nitric oxide inhibitory potential of Curcuma angustifolia Roxb. essential oil: An in silico and *in vitro* analysis. Plant Sci Today 2024;11(4):234-43. https://doi.org/10.14719/pst.3410

13. Nordin A, Saim AB, Ramli R, Hamid AA, Nasri NWM, Idrus RBH. Miswak and oral health: An evidence-based review. Saudi J Biol Sci 2020;27(7):1801-10. (PMID: 32565699)

14. Azab A, Nassar A, Azab AN. Anti-inflammatory activity of natural products. Molecules 2016;21:1321. (PMID: 27706084)

15. Garcin ED, Arvai AS, Rosenfeld RJ, et al. Anchored plasticity opens doors for selective inhibitor design in nitric oxide synthase. Nat Chem Biol 2008;4:700-7. (PMID: 18849972)

16. Xu J, Peng M, Sun X, et al. Bioactive diterpenoids from Trigonostemon chinensis: structures, NO inhibitory activities, and interactions with iNOS. Bioorg Med Chem Lett 2016;26:4785-9. (PMID: 27570243)

17. Chayah M, Carrión MD, Gallo MA, Jiménez R, Duarte J, Camacho ME. Development of urea and thiourea kynurenamine derivatives: synthesis, molecular modeling, and biological evaluation as nitric oxide synthase inhibitors. ChemMedChem 2015;10:874-82. (PMID: 25801086)

18. Eftekhari SA, Toghraie D, Hekmatifar M, Sabetvand R. Mechanical and thermal stability of armchair and zig-zag carbon sheets using classical MD simulation with Tersoff potential. Phys E Low Dimens Syst Nanostruct 2021;133:114789. https://doi.org/10.1016/j.physe.2021.114789

19. Nayak A, Gadnayak A, Dash KT, et al. Exploring molecular docking with MM-GBSA and molecular dynamics simulation to predict potent inhibitors of cyclooxygenase (COX-2) enzyme from terpenoid-based active principles of Zingiber species. J Biomol Struct Dyn 2023 Dec;41(20):10840-50. (PMID: 36576262)

20. García-Aranda MI, Gonzalez-Padilla JE, Gómez-Castro CZ, et al. Anti-inflammatory effect and inhibition of nitric oxide production by targeting COXs and iNOS enzymes with the 1,2-diphenylbenzimidazole pharmacophore. Bioorg Med Chem 2020;28:115427. (PMID: 32205045)

21. Chen Y, Zhang F, Sun J, Zhang L. Identifying the natural products in the treatment of atherosclerosis by increasing HDL-C level based on bioinformatics analysis, molecular docking, and *in vitro* experiment. J Transl Med 2023;21:920. (PMID: 38115108)